

## Supplementary Information:

### DNA Encapsulation of Ten Silver Atoms Producing a Bright, Modulatable, Near-Infrared-Emitting Cluster

*Jeffrey T. Petty,\*<sup>1</sup> Chaoyang Fan,<sup>2</sup> Sandra P. Story,<sup>1</sup> Bidisha Sengupta,<sup>1</sup> Ashlee St. John Iyer,<sup>2</sup> Zachary Prudowsky,<sup>1</sup> and Robert M. Dickson\*<sup>2</sup>*

<sup>1</sup>Department of Chemistry, Furman University, Greenville, SC 29613

<sup>2</sup>School of Chemistry and Biochemistry and Petit Institute for Bioengineering and Bioscience, Georgia Institute of Technology, Atlanta, GA 30332

#### Experimental Methods

Silver nitrate (Aldrich, 99.9999%) and sodium borohydride (Aldrich, 99%) were used as received. The oligonucleotide C<sub>3</sub>AC<sub>3</sub>AC<sub>3</sub>TC<sub>3</sub>A (Integrated DNA Technologies) was purified by desalting by the manufacturer and dissolved in sterilized, deionized water (Barnstead Nanopure ultrapure water system). Concentrations were determined by absorbance using molar absorptivities based on the nearest-neighbor approximation.<sup>1</sup> Silver nanoclusters were synthesized by adding stock aqueous 1 mM oligonucleotide and 6 mM Ag<sup>+</sup> solutions to a 10 mM citrate buffer at pH = 7 to give final concentrations of 15 and 120 μM, respectively. After 15 sec of mixing, a 20 mM stock solution of BH<sub>4</sub><sup>-</sup> was added to give a final concentration of 60 μM, and the resulting solution was vigorously shaken for 1 min. Temperature can influence the maxima in the absorption, excitation, and emission spectra by ~20 nm. Samples for elemental analysis were prepared at room temperature to maintain consistent treatment and spectra throughout the preparation and analysis. The samples were allowed to react overnight in the dark prior to analysis. The species is most stable in citrate but can also be formed in cacodylate and presumably other buffer solutions. No fluorescence is observed when Ag<sup>+</sup> is reduced in the absence of DNA.

Visible absorption spectra were acquired using a Varian Cary 50 Bio UV-Visible and a Shimadzu UV-2401 PC spectrophotometer. Circular dichroism spectra were obtained from a

Jasco J-710 spectropolarimeter. Fluorescence spectra were acquired on Jobin Yvon Horiba Fluoromax-3 and Photon Technology International QuantaMaster spectrofluorimeters. Correspondence between the excitation and absorbance bands in the near infrared allowed the fluorescence quantum yield to be measured using Cy7 ( $\Phi_f = 0.13$ ) as the reference chromophore.<sup>2,3</sup> Reversed-phase ion-pair chromatography was performed with a Shimadzu Prominence HPLC system using a semi-prep Gemini C18 column, which is 50 mm long and 10 mm internal diameter and has particles with an average size of 5  $\mu\text{m}$  and a pore size of 110  $\text{\AA}$  (Phenomenex). The mobile phase was 35 mM triethylamine acetate at pH = 7 and methanol, with a linear gradient of 10%-30% methanol over 8 min followed by a 3 min hold at 10% methanol at a flow rate of 5 mL/min. Separations were conducted at 25 °C. Absorbance and fluorescence measurements of the separated species were made using the SPD-M20A and RF-10XL, respectively. Using a FRC-10A fraction collector, the solutions containing the isolated cluster-DNA conjugate were dehydrated and dissolved in water containing 5% nitric acid. After HPLC purification, the quantities of silver and phosphorous were determined by inductively coupled plasma-atomic emission spectroscopy (Optima 7300 DV, Perkin Elmer). To account for different detection efficiencies, control samples comprised of known relative amounts  $\text{Ag}^+$  and  $\text{C}_3\text{AC}_3\text{AC}_3\text{TC}_3\text{A}$  were used. To determine the oligonucleotide concentration, the stoichiometry of 15 phosphorous:oligonucleotide was used, which accounts for the absent terminal 3'-phosphate.

Fluorescence correlation spectroscopy studies were conducted using excitation at 730 nm with a cw power of  $\sim 30 \mu\text{W}$  provided by a Ti:Sapphire laser (Coherent Mira 900). A 60x 1.2 NA water immersion microscope objective (UPLAN S APO, Olympus) was used in a laser epi-illuminated geometry to excite the sample and collect the fluorescence emission. A long-pass dichroic (Semrock) was used to reflect the 730 nm excitation into the back of the objective and transmit the emission, which was passed through a 760 nm long-pass filter to a 50  $\mu\text{m}$  diameter fiber located at the image plane of the microscope. The fiber was coupled with an

actively-quenched single-photon counting avalanche photodiode (APD) detector (SPCM-AQR14, Perkin Elmer). The TTL APD output signal was split (Pulse Research Labs) and sent to both a counting board (National Instruments) and to a hardware correlator (Correlator.com). Sample droplets were placed on a glass cover slip for analysis.

A dilute solution of the Cy7 (D1421, GE Lifesciences) in buffer was used as a reference fluorophore to determine the dimensions of the probe volume using a 3-D Gaussian model:<sup>4</sup>

$$G(\tau) = 1 + \frac{1}{N} \left( 1 + \frac{\tau}{\tau_d} \right)^{-1} \left( 1 + \left( \frac{\omega}{z} \right)^2 \left( \frac{\tau}{\tau_d} \right) \right)^{-\frac{1}{2}}$$

In this equation,  $G(\tau)$  is the fluorescence intensity autocorrelation,  $\tau$  is the lag time,  $N$  is the average number of fluorescent species in the probe volume,  $\omega$  is the transverse radius of the probe volume,  $z$  is the height of the probe volume, and  $\tau_d$  is the lag time at which the autocorrelation amplitude has decayed to approximately one half of its maximum value,  $G(0)$ . The aspect ratio  $\omega/z$  was set to 10 for the measurements. The probe volume radius is related to the crossing time and the translational diffusion coefficient ( $D$ ) by:

$$\omega = \sqrt{4D\tau_d}$$

The diffusion coefficient for Cy7 was estimated to be  $3.2 \times 10^{-6} \text{ cm}^2/\text{s}$  based on the diffusion coefficient of  $3.7 (\pm 0.2) \times 10^{-6} \text{ cm}^2/\text{s}$  for Cy5 and accounting for an increase of 1 Å for the hydrodynamic radius of Cy7 relative to Cy5.<sup>5</sup> Assuming a spherical particle, the Stokes-Einstein relationship is used to relate the diffusion coefficient to the hydrodynamic radius ( $r$ ):

$$D = \frac{kT}{6\pi\eta r}$$

in which  $k$  is the Boltzmann constant,  $T$  is the temperature, and  $\eta$  is the solution viscosity.

For fluorescence imaging, clusters and Cy7 were dissolved in 4% (w/v) polyvinyl alcohol in water and spin cast onto clean glass coverslips (22.5 x 22.5 x 0.15 mm, Fisher). An inverted microscope (IX70, Olympus) with a 100X (1.4 NA) oil immersion objective was used. The output of a mercury lamp was directed through the back port of the microscope, filtered with a 670 – 740 nm bandpass filter, and reflected into the objective that focused the light onto the sample. The dichroic was chosen to maximize the reflectance of the excitation wavelength while efficiently passing the emission. The emission collected by the objective was passed through a 760 nm long-pass filter and directed to the side port for detection by a CCD camera (IXON, Andor). Data was collected in 2-s bins. Photostability in solution was evaluated by irradiating Cy7 and cluster-DNA samples with a 2 mW diode laser operating at 690 nm with a 1 mm beam diameter. Concentrations of both Cy7 and the silver cluster were adjusted to yield initial fluorescence intensities of ~200 kHz for each sample using 690-nm excitation at and detecting emission at 770 and 795 nm, respectively. The samples were stirred during irradiation. Their fluorescence spectra were periodically monitored in a PTI Quantamaster fluorometer over a 2-hour time period.

Dual wavelength excitation of the clusters used two diode lasers operating at 690 nm and 905 nm (HL6738MG and L904P030, ThorLabs) whose current and temperature were controlled (LTC100, Thorlabs). The intensity of the longer wavelength laser was modulated using a mechanical chopper operated at 4.3 Hz. The two lasers were spatially overlapped via a dichroic mirror and were routed through the back port of the microscope. A dichroic in the microscope reflected the two lasers into the objective while efficiently passing the collected emission. Further discrimination of the cluster emission was accomplished using 760 nm long-pass and 850 nm short-pass filters. Emitted light was then passed to the side port and spatially filtered by a 100- $\mu$ m pinhole at the conjugate image plane. Detection was accomplished using an APD, and the signal was processed with a digital counting board (PCI-6602, National

Instruments) using 0.01 s bins. Fourier analysis of the signal was accomplished using Origin 7.5.

The fluorescence lifetime was measured using a mode-locked Ti-Sapphire laser operating at 730 nm (Coherent Mira). The signal was detected using an APD and processed with a photon counting module (SPC-630, Becker Hickl). Fluorescence decays accounted for convolution of the fluorescence decay with the instrument response function.

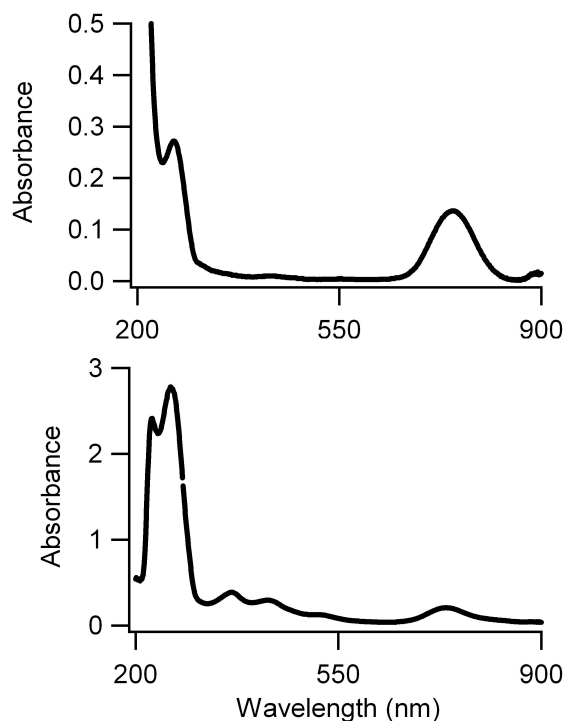


Figure 1S: Absorption spectra of purified (top) and unpurified (bottom) silver clusters. The purified sample was obtained by collecting the sample corresponding to Peak II in Figure 3.

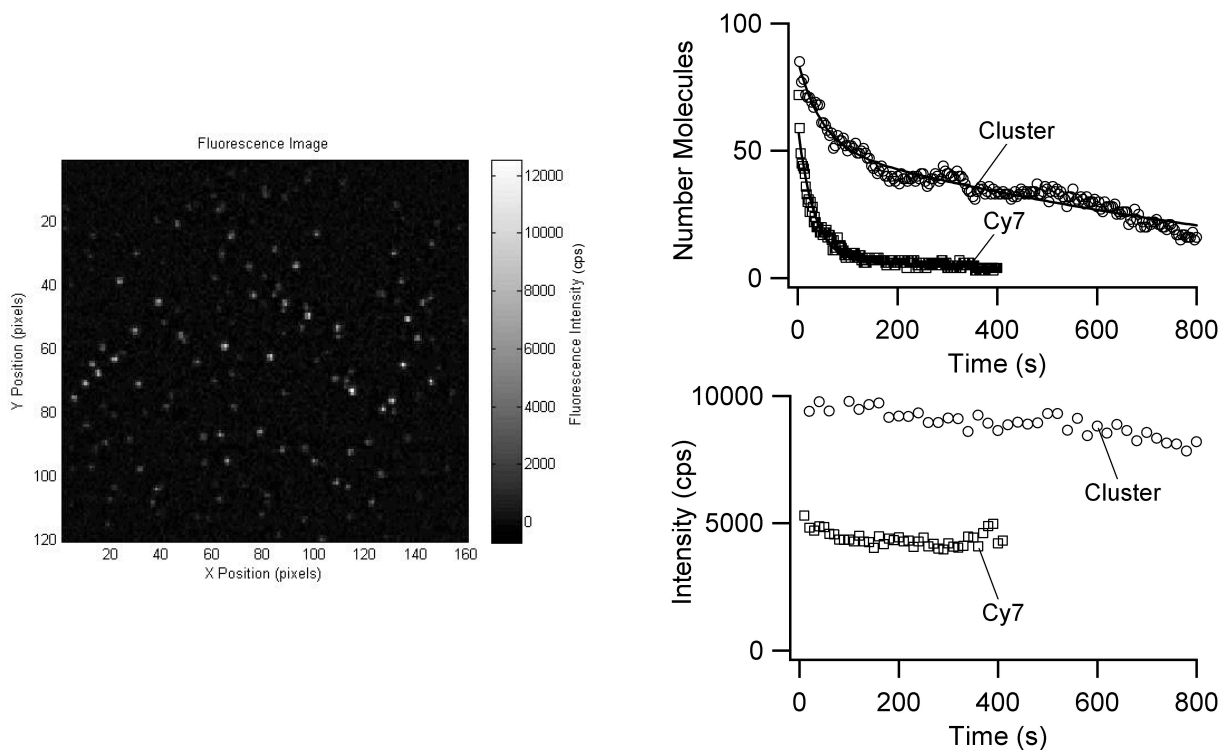


Fig. 2S (Left) Fluorescence image acquired using mercury lamp excitation for a sample of isolated silver clusters in polyvinyl alcohol. (Right, top) A comparison of the survival times of silver clusters and Cy7. (Right, bottom) Average intensity (counts/sec) per cluster and per Cy7 molecule using data from the above figure.

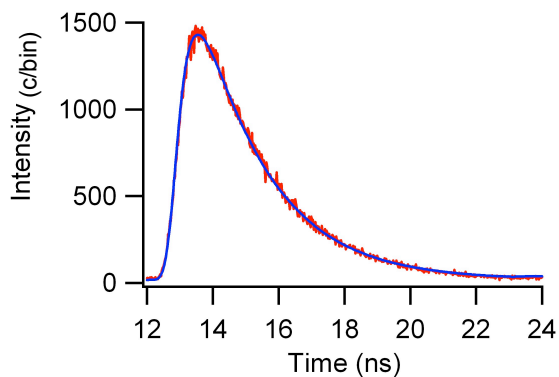


Fig. 3S Time-dependent intensity changes (counts/bin) in red to determine the fluorescence lifetime of the silver clusters. The fit in blue accounts for the instrument response.

---

<sup>1</sup> Bloomfield, V. A.; Crothers, D. M.; Tinoco, J., Ignacio, Nucleic Acids: Structures, Properties, and Functions. ed.; University Science Books: Sausalito, CA, 2000; p. 794.

---

<sup>2</sup> Williams, A. T. R.; Winfield, S. A.; Miller, J. N., Relative Fluorescence Quantum Yields Using a Computer-Controlled Luminescence Spectrometer. *Analyst* 1983, 108, (1290), 1067-1071.

<sup>3</sup> Texier, I.; Goutayer, M.; Da Silva, A.; Guyon, L.; Djaker, N.; Josserand, V.; Neumann, E.; Bibette, J.; Vinet, F., Cyanine-loaded lipid nanoparticles for improved in vivo fluorescence imaging. *Journal of Biomedical Optics* 2009, 14, (5), 054005.

<sup>4</sup> Rigler, R., U. Mets, et al. (1993). "Fluorescence Correlation Spectroscopy With High Count Rate and Low Background: Analysis of Translational Diffusion." *Eur. Biophys. J.* 22: 169-175.

<sup>5</sup> Loman, A.; Dertinger, T.; Koberling, F.; Enderlein, J., Comparison of optical saturation effects in conventional and dual-focus fluorescence correlation spectroscopy. *Chemical Physics Letters* 2008, 459, (1-6), 18-21.